Published in final edited form as:
Clin Cancer Res. 2008 July 15; 14(14): . doi:10.1158/1078-0432.CCR-07-5243.

Analysis and Reproducibility of 3′-Deoxy-3′-[^{18}F]Fluorothymidine Positron Emission Tomography Imaging in Patients with Non - Small Cell Lung Cancer

Anthony F. Shields[1,2], **Jawana M. Lawhorn-Crews**[1,2], **David A. Briston**[1,2], **Sajad Zalzala**[1,2], **Shirish Gadgeel**[1,2], **Kirk A. Douglas**[1,2], **Thomas J. Mangner**[1,3], **Lance K. Heilbrun**[1,2], and **Otto Muzik**[1,4]

[1]Karmanos Cancer Institute, Wayne State University, Detroit, Michigan

[2]Department of Internal Medicine, Wayne State University, Detroit, Michigan

[3]Department of Radiology, Wayne State University, Detroit, Michigan

[4]Department of Pediatrics, Wayne State University, Detroit, Michigan

Abstract

Purpose—Imaging tumor proliferation with 3′-deoxy-3′-[^{18}F]fluorothymidine (FLT) and positron emission tomography is being developed with the goal of monitoring antineoplastic therapy. This study assessed the methods to measure FLT retention in patients with non-small cell lung cancer (NSCLC) to measure the reproducibility of this approach.

Experimental Design—Nine patients with NSCLC who were untreated or had progressed after previous therapy were imaged twice using FLT and positron emission tomography within 2 to 7 days. Reproducibility (that is, error) was measured as the percent difference between the two patient scans. Dynamic imaging was obtained during the first 60 min after injection. Activity in the blood was assessed from aortic images and the fraction of unmetabolized FLT was measured. Regions of interest were drawn on the plane with the highest activity and the adjacent planes to measure standardized uptake value (SUV_{mean}) and kinetic variables of FLT flux.

Results—We found that the SUV_{mean} obtained from 30 to 60 min had a mean error of 3.6% (range, 0.6–6.9%; SD, 2.3%) and the first and second scans were highly correlated ($r^2 = 0.99$; $P < 0.0001$). Using shorter imaging times from 25 to 30 min or from 55 to 60 min postinjection also resulted in small error rates; SUV_{mean} mean errors were 8.4% and 5.7%, respectively. Compartmental and graphical kinetic analyses were also fairly reproducible ($r^2 = 0.59$; $P = 0.0152$ and $r^2 = 0.58$; $P = 0.0175$ respectively).

Conclusion—FLT imaging of patients with NSCLC was quite reproducible with a worst case SUV_{mean} error of 21% when using a short imaging time.

For positron emission tomography to be useful in the evaluation of tumor response to therapy, one must be able to measure important aspects of tumor metabolism quantitatively and reproducibly. Depending on the tracer employed, one can assess different metabolic

Requests for reprints: Anthony F. Shields, Karmanos Cancer Institute, Wayne State University, 4100 John R. Street, 4 HWCRC, Detroit, MI 48201-2013. Phone: 313-576-8735; Fax: 313-576-8767; ShieldsA@Karmanos.org.

Grant support: National Cancer Institute grants CA39566 and CA 22453.

Disclosure of Potential Conflicts of Interest
No potential conflicts of interest were disclosed.

pathways, which may vary in utility depending on the tumor being imaged, the location in the body, and the treatment used. The most commonly used agent in oncology has been fluorodeoxyglucose (FDG; ref. (1)), but new tracers that measure proliferation may offer improved assessment of response. This is particularly likely in the assessment of new, targeted agents that may interfere with oncogenic pathways and hence may simply turn off the cell growth. Measuring proliferation may also yield an early indication of response, because DNA synthesis may decline before cellular energetics. Although [^{11}C]thymidine can reproducibly measure DNA synthesis and treatment response, it has practical limitations owing to the short half-life of ^{11}C and the rapid catabolism of thymidine (2–5). Thymidine analogues labeled with ^{18}F have been developed that also resist catabolism (6–8). Of these, 3′-deoxy-3′-[^{18}F]fluorothymidine (FLT) has received the most study (9). For any tracer to be useful in response assessment, its analysis must be accomplished in a reproducible manner.

FDG has gained widespread use in the detection and staging of cancer and has been studied for use in evaluating response to treatment in several tumor types (10). Measurement of tumor metabolism with FDG has generally been accomplished through the use of the standardized uptake value (SUV). Two small studies have examined the reproducibility of FDG in patients with untreated lung cancer and found errors of <20% (11, 12). As we have sought to develop FLT for imaging tumor response, it is also necessary to determine the best way to measure FLT retention, including SUV and kinetic variables, and to determine the reproducibility in several tumor types. In this study, we have examined the reproducibility of FLT imaging in patients with advanced non-small cell lung cancer (NSCLC).

Materials and Methods

Patient characteristics

Nine patients with NSCLC were included in our study and had two FLT positron emission tomography scans a mean of 6.5 days apart (range, 2–7 days). The patients ranged in age from 45.8 to 68.0 years (mean, 60.5), with four males and five females. Six of the patients had recently diagnosed stage III to IV disease, five of which had never received previous therapy and one had surgery and radiotherapy for brain metastases. Of the three patients with earlier diagnoses, one had chemotherapy 3 months before imaging and had recent progression and another two patients had progressed after chemoradiotherapy, which was completed at least 11 months before imaging. Two additional patients had been enrolled on the study but not included in this analysis, because, on review, one was found to have completed a prolonged course of radiotherapy 1month before imaging and the other required treatment with zolendronic acid for hypercalcemia between scans 1and 2. The Wayne State University Institutional Review Board and Radioactive Drug Research Committee approved the study and a signed informed consent was obtained from each patient before the first scan.

Radiochemistry and image acquisition

The synthesis of FLT was accomplished using the methods of Grierson and Shields (13) and Machulla (14) with a purity of >98.0% and with a specific activity of at least 210 GBq/Amol. All patients were imaged in a supine position on a CTI/Siemens ECAT/HR Tomograph, which acquires 47 image planes with a 3.2 mm plane thickness. Before imaging, two small i.v. catheters were placed in opposite arms for tracer injection and blood sampling. Subsequently, a 20-min attenuation correction was done at the location of the tumor. To allow adequate temporal sampling of the input function, the FLT tracer was administered as an i.v. infusion over 60 s (1min) after the onset of dynamic imaging. Patients received a mean of 373 MBq FLT (range, 292–389). The dynamic image sequence

consisted of 25 frames over 60 min (1 × 60 s, 4 × 20 s, 4 × 40 s, 4 × 60 s, 4 × 180 s, and 8 × 300 s). The images were reconstructed using a filtered back-projection algorithm applying a Hanning filter with a smoothing kernel of 13 mm full-width at half-maximum. The amount of FLT metabolized into its glucuronide was determined from a blood sample obtained 60 min after FLT injection using a two-step column, and the fraction of intact FLT at each time point was estimated by interpolation as described previously (15).

Image analysis

Image analysis was done using computer programs developed in IDL (ITT Visual Information Solutions) and the Clinical Application Programming Package (CTI/Siemens). Tumors were visually identified and confirmed with either computed tomography or magnetic resonance imaging scans. The plane of the tumor with the ‘‘hottest’’ pixel was identified and it, along with the two adjacent planes, was used for analysis. Furthermore, to objectively determine the mean tumor SUV value (SUV_{mean}), the software determined an isocontour at the level of activity half-way between the most active pixel in the tumor and a background region of interest (ROI; defined separately). The SUV_{mean}, SUV_{max}, and SUV_{peak} (1cm diameter ROI around SUV_{max}) were determined in three consecutive planes and were averaged. This procedure was initially done on summed images 30 to 60 min postinjection and subsequently repeated on summed images 25 to 30 and 55 to 60 min postinjection.

Blood time-activity curves data were obtained from 1-h dynamic images by measuring SUV_{mean} on a 3.0 cm diameter circle over the descending thoracic aorta in three consecutive planes. The mean value was calculated and applied to all the frames in the 1-h dynamic images. Total blood activity was multiplied by the percentage of activity in unmetabolized FLT, as we have described previously, and this was used as the blood input function for kinetic analysis (15). Dynamic data for the tumor were obtained by applying the mean ROI drawn on the 30 to 60 min summed image to the rest of the image data.

Kinetic modeling

A three-compartment model as well as the Patlak graphical approach were used for kinetic analysis of time-activity curves. Input variables for compartmental modeling used starting values of K_1 = 0.20 mL/min/g, k_2 = 0.10 min^{-1}, k_3 = 0.035 min^{-1}, and k_4 = 0.0 min^{-1}. Nonlinear fitting was initially done with k_4 set to zero and subsequently allowing k_4 to float. In all fits, the blood volume was set to 5%. Nonlinear regression was done using a Marquardt-Levenberg least-squares algorithm yielding estimates for the kinetic variables K_1 to k_4. Based on the fitted values, FLT flux was calculated as $K_1 \times k_3 / (k_2 + k_3)$ mL/min/g. The Patlak graphical approach used the time interval between 5 and 60 min.

Statistical methods

Statistical methods included descriptive statistics and graphics (box plots and scatter plots). Reproducibility (that is, error) was measured as the percent difference between the two patient scans: % difference = 100 × ABS (scan 2 − scan 1) / [(scan 1 + scan 2) / 2]. This difference was calculated for SUV_{mean}, SUV_{peak}, SUV_{max}, and (for the kinetic analysis) area under the curve. The graphical analysis included bivariate scatter plots and Pearson correlations (r). Linear regressions reported slope, intercept, and r^2 values to characterize the association between scans 1and 2. A similar statistical approach was used to compare imaging time intervals or to compare analysis methods. When comparing analysis methods, the regression models were fit separately to scan 1data and scan 2 data. This assures statistical independence of the observations for each regression model.

Results

SUV measurements

Nine patients with advanced NSCLC were imaged twice and the uptake of FLT was measured in the tumors using several different variables. SUV_{mean}, SUV_{peak}, and SUV_{max} were determined independently in each scan. We initially drew the ROI on the summed images obtained from 30 to 60 min after FLT infusion. It was found that the SUV_{mean} from 30 to 60 min was highly reproducible with a mean error of 3.6% (range, 0.6–6.9%; SD, 2.3%) and the first and second scans were highly correlated ($r^2 = 0.99$; $P < 0.0001$; Table 1; Figs. 1 and 2). SUV_{peak} and SUV_{max} had mean errors of 4.6% (range, 1.7–10.2%; SD, 3.4%) and 5.3% (range, 0.8–15.2%; SD, 4.8%), respectively, when drawn on the 30 to 60 min images.

Because the image data from 30 to 60 min postinjection are only obtained when a dynamic scan is done, we also evaluated the reproducibility of SUV measures obtained from shorter intervals as might be obtained as part of a single positron emission tomography/computed tomography whole-body scan. Using SUV_{mean} values derived from summed images between 25 to 30 and 55 to 60 min postinjection, the mean error was found to be 8.3% (range, 0.5–20.9%; SD, 6.9%) and 5.7% (range, 0.1–13.0%; SD, 4.5%), respectively (Table 1; Fig. 2). The two measurements using either time interval correlated well with $r^2 = 0.94$, $P < 0.0001$and $r^2 = 0.95$, $P < 0.0001$for both SUV_{mean} obtained at 25 to 30 and 55 to 60 min, respectively.

It was also noted that comparing the measurements obtained from 30 to 60 min also correlated well with those obtained over the shorter intervals. Each patient was imaged twice, so when fitting a regression model to measurements made within a single scan, we initially used just the scan 1images. We then did the same analysis on the images obtained as part of scan 2. SUV_{mean} measured from scan 1at 30 to 60 min was well correlated with the 55 to 60 min ($r^2 = 0.97$; $P < 0.0001$) measurement and the 25 to 30 min ($r^2 = 0.93$; $P < 0.0001$) measurement (Fig. 3A and B). Almost identical results were seen with a similar regression model fit for scan 2 (Fig. 3). In summary, either of these approaches produces sufficiently accurate measurements such that one may use shorter imaging times.

Finally, we also observed a high correlation between SUV_{mean} values derived from summed images between 25 and 30 min (x) and 55 and 60 min (y) postinjection ($r^2 = 0.92$; $P < 0.0001$; $y = 1.028x + 0.02$; Fig. 3C). This indicates that the SUV_{mean} values are largely independent from the exact timing of summed images, which might be relevant for routine clinical scans where the exact time of imaging might vary slightly from patient to patient and scan to scan.

Dynamic measurements

Kinetic measurement of FLT retention was obtained using the full dynamic curve from the ROI drawn for the SUV_{mean} along with a blood input function drawn on the aorta. For graphical and compartmental analyses, the regression of scan 2 on scan 1yielded $r^2 = 0.58$, $P = 0.0175$ and $r^2 = 0.59$, $P = 0.0152$, respectively. Furthermore, the graphical and compartmental approaches correlated well with each other ($r^2 = 0.85$; $P < 0.0004$ for scan 1; Fig. 4). We found that the mean error using the Patlak graphical approach was 28.5% (range, 9.2–68.0%; SD, 17.5%), and using the three-compartment model (with $k_4 = 0$), it was 25.1% (range, 5.5–57.9%; SD, 15.6%; Table 2; Fig. 1). Allowing k_4 to float increased the variability to a mean error of 36.6% (range, 4.7–136.5%; SD, 43.7%); hence, our principal analyses set k_4 to zero. Comparing the compartmental analysis with SUV_{mean} (30–60 min) gave a reasonable correlation result ($r^2 = 0.72$; P < 0.0040 for scan 1).

Catabolism and clearance of FLT

Because there was higher variation using dynamic analysis compared with that obtained using the SUV, we analyzed the source of the differences. First, we examined the fraction of intact FLT and metabolites found by analysis of blood obtained at 60 min after injection. We found that the mean difference between scans 1and 2 was 2.3% (range, 0.2–4.4%; SD, 1.2%) despite a range between patients of 65.3% to 85.1% found in intact FLT. Our previous study has shown that using the two-step column had a mean error of 1.2% when the same sample was assayed repeatedly (15). Our results obtained from the same patient imaged days apart show that the metabolism of FLT varies little in patients who were untreated or not recently treated.

Another potential source of error is the reproducibility of the blood input function obtained from a ROI defined on the descending aorta. To assess the reproducibility of this measurement, we quantitated the area under the blood activity curve for different intervals. We did find that the blood area under the curve varied from scans 1to 2 with a mean error of 24.0% (range, 0.8–36.4%; SD, 18.9%). Hence, differences in the blood curves could account for some of the differences in the kinetic variables seen between scans 1and 2. However, a closer inspection of the differences observed between the graphical and the compartmental approaches showed that the errors varied from one technique to the other even in the same patient. These results indicate that the errors in the kinetic variables are the result of noise in the dynamic blood and tumor curves.

Discussion

FLT was developed to provide a measure of tumor proliferation because it is taken up by cells and retained after phosphorylation by thymidine kinase 1. Thymidine kinase 1 increases as cells enter the DNA synthetic phase, and previous work has shown that FLT retention generally correlates with other measures of tumor proliferation. The most likely use of FLT will be in monitoring treatment response, but such studies need to consider the different methods for measuring FLT retention in tumors and their reproducibility.

The most common method of measuring tracer retention has been through the use of the semiquantitative approach of the SUV. The SUV uses the measurement of activity within a ROI along with the injected dose and the weight of the patient to calculate the desired variable. To take into account differences in the proportion of fat in patients, some investigators have adjusted the SUV by using lean body mass, ideal body weight, or even body surface area. When studying the reproducibility of FLT measurements, we deemed these modifications unnecessary, because over the course of ~ 1week these correction factors would not have changed. If one was following SUV over many months and there was a marked change in patient weight, such corrections might be useful.

Two small previous studies have examined the reproducibility of the glucose analogue FDG when used in patients with NSCLC (11, 12) and another study examined the reproducibility in lung and breast cancer (16). Each of these studies found that when no treatment was used the difference between scans was generally <20%. A larger, multicenter trial to examine the reproducibility of FDG imaging in NSCLC is now under way under the sponsorship of the American College of Radiology Imaging Network and they plan to enroll ~ 60 patients to examine this question. A study of FLT in nine mice with tumor xenografts found a (mean ± SD) 14 ± 10% coefficient of variation in replicate scans as measured by the percent injected dose per gram (17). One study has examined the change in FLT retention after the treatment of breast cancer and reported the reproducibility in 9 patients before treatment (18). This study by Kenny et al. found that the SD of the mean percent difference between the two scans was 10.5% and 15.1% for measurements of the SUV and FLT flux measured by

graphical analysis, respectively. Their regression analysis showed correlation coefficients of $r = 0.99$ and 0.97 for SUV and FLT flux measurements, respectively. Although our SUV measurements were highly correlated, for example, $SUV_{mean} r^2 = 0.99$; $P < 0.0001$, our Patlak measurements were not quite as well correlated ($r^2 = 0.58$; $P = 0.0175$). Part of this difference might be attributed to the use of direct arterial sampling to obtain the blood input function in the study by Kenny et al., whereas we used imaging of the aorta to measure the blood activity. They also imaged the patients for 95 min to obtain the kinetic curves, whereas we limited our dynamic imaging to 60 min.

In the present study, patients with NSCLC were studied with two FLT scans before any treatment or after progression in the chest. We measured the SUV using three different approaches to determine the ROI and used different time frames. To measure the SUV_{mean}, we employed a semiautomated method to define the border of the ROI as the isocontour value that reflects the mean of the maximum SUV in the tumor and the background. There is no accepted standard method for drawing the ROI, but investigators generally use freehand drawing and thresholding approaches (19). The approach we have chosen gave very reasonable results, but we showed similar results with any of the commonly used approaches, such as SUV_{peak} and SUV_{max}. Although the SUV_{peak} measures only a small part of large tumors, because it just includes a circle of ~ 1cm drawn around the maximum pixel, one does not have to determine the border of the tumor. The other approach that is commonly used is to measure the hottest pixel or SUV_{max}, which we have averaged over the three adjacent planes to decrease noise. This is certainly the simplest method to quantitate tumor activity but introduces slightly more variability as seen in our results. Until further multicenter studies are done, it is suggested that studies include each of these approaches.

In our previous work and in this study, we initially obtained our SUV measurements on an image summed from 30 to 60 min postinjection. This has the benefit of minimizing noise and was easy for us to perform because we were obtaining a dynamic image for the first 60 min postinjection. If the investigator was just going to obtain a static image, as is regularly done using positron emission tomography/computed tomography in clinical studies, then the emission scan may be limited to a few minutes. To examine this situation, we analyzed the reproducibility of scans obtained from 55 to 60 min postinjection and found a mean error of 5.7% (range, 0.1–13.0%; SD, 4.5%). Because image acquisition was started with the injection of the FLT, the timing of our images postinjection was precise. For a regular clinical scan, the injection might be done in another room and the patient would then be moved into the scanner at a designated time postinjection. This can lead to some variability in the timing of image acquisition. For example, the present American College of Radiology Imaging Network 6678 trial using FDG requires that the first scan be started between 50 and 70 min after tracer injection and that subsequent scans are matched in timing to the first scan within 10 min. To determine if variability in the start of imaging might affect the reproducibility of the results in static imaging, we compared images obtained at 25 to 30 and 55 to 60 min postinjection and found that they were well correlated ($r^2 = 0.92$; $P < 0.0001$). This shows that these patients had reached a plateau in FLT retention by 30 min, but this issue would also need to be considered for other tumor types and after therapy, where kinetics might vary.

Although further studies of FLT reproducibility are needed, one can use the data from this present study and that of Kenny et al. to begin to formulate some guidelines (18). In both studies, larger ROI were drawn around the tumor either manually or using a semiautomated threshold approach, which included most of the tumor. When measuring a SUV, they obtained the images over 10 min, whereas we have shown that 5 min of emission acquisition provided reasonable results. Kenny et al. reported that the SD of the mean percent difference was 10.5% between scans (but did not report a maximum). Assuming distributional

normality, their SD is roughly comparable with our observed maximum difference in all our SUV_{mean} measurements of 20.9%. This would lead one to suggest that scans with a SUV_{mean} differing by >25% are likely to reflect true treatment differences. Clearly, further studies of this issue, including multicenter trials, are required.

The other important method of tracer quantitation makes use of the full dynamic curve of FLT retention in the tumor, measurements of total blood activity, and the fraction of intact FLT in the blood. Although SUV measurements are relatively simple, they do not take into account changes in tracer clearance in the blood or possible changes in the tumor metabolism. Dynamic measurements can overcome some of these issues but are more complex to obtain, and one can introduce additional sources of noise into the variable estimation. We measured FLT retention for 60 min after injection and fit the results using a standard three-compartment model and a graphical approach. It should be noted that k_4 is the variable that represents dephosphorylation of FLT phosphate and we initially set k_4 to zero. We have found previously that we could not estimate k_4 with 60 min of imaging data (15). In this study, we also studied kinetic measurements allowing k_4 to float but found that it decreased the reproducibility of our measurements. Although other investigators have reported that k_4 is not zero, ~120 min of dynamic data were required to accurately estimate this variable (20). Such a long imaging time is not considered practical for most clinical studies, but the shorter imaging time may contribute to some of the errors we noted. We also used ROI over the aorta to estimate the blood time activity curve and it is likely that one might improve the accuracy using arterial blood sampling, although this is not going to be possible in many trials.

Overall, we found that the methods we employed produced reasonably reproducible measurements from the dynamic data, but they had greater errors than those seen with SUV alone. The real issue is does kinetic measurement assist in quantitating treatment response. For example, if treatment with multiagent chemotherapy changed FLT clearance, we might find that dynamic measurements, although somewhat less precise, provide a more accurate measure of tumor response. Further studies will need to compare these approaches in patients who are undergoing treatment.

Conclusions

The results obtained in nine patients with NSCLC show that measurement of FLT is reproducible with errors comparable with those seen with FDG. SUV measurements can be obtained using ROI drawn to represent the whole tumor, the peak, or the area of maximum activity with time intervals as short as 5 min. Although kinetic measurements could be obtained with acceptable mean errors, the range of errors was higher than that seen with SUV.

References

1. Weber WA. Use of PET for monitoring cancer therapy and for predicting outcome. J Nucl Med. 2005; 46:983–95. [PubMed: 15937310]
2. Gunn RN, Yap JT, Wells P, et al. A general method to correct PET data for tissue metabolites using a dualscan approach. J Nucl Med. 2000; 41:706–11. [PubMed: 10768573]
3. Shields AF, Graham MM, Kozawa SM, et al. Contribution of labeled carbon dioxide to PET imaging of carbon-11-labeled compounds. J Nucl Med. 1992; 33:581–4. [PubMed: 1552344]
4. Shields AF, Mankoff DA, Link JM, et al. [^{11} C]thymidine and FDG to measure therapy response. J Nucl Med. 1998; 39:1757–62. [PubMed: 9776283]
5. Wells P, Gunn RN, Steel C, et al. 2-[^{11}C]thymidine positron emission tomography reproducibility in humans. Clin Cancer Res. 2005; 11:4341–7. [PubMed: 15958616]

6. Conti P, Alauddin M, Fissekis J, Schmall B, Watanabe K. Synthesis of 2′-fluoro-5-[^{11}C]-methyl-1-β-D-arabi-nofuranosyluracil ([^{11}C]-FMAU): a potential nucleoside analog for in vivo study of cellular proliferation with PET. Nucl Med Biol. 1995; 22:783–9. [PubMed: 8535339]
7. Shields A, Grierson J, Dohmen B, et al. Imaging proliferation in vivo with [F-18]FLT and positron emission tomography. Nat Med. 1998; 4:1334–6. [PubMed: 9809561]
8. Sun H, Sloan A, Mangner TJ, et al. Imaging DNA synthesis with [^{18} F]FMAU and positron emission tomography in patients with cancer. Eur J Nucl Med Mol Imaging. 2005; 32:15–22. [PubMed: 15586282]
9. Bading JR, Shields AF. Imaging cell proliferation : status and prospects. J Nucl Med. 2008; 49:64S–80S. [PubMed: 18523066]
10. Weber, WA. [^{18}F]Fluorodeoxyglucose positron emission tomography assessment of response. In: Shields, AF.; Price, P., editors. *In vivo* imaging of cancer therapy. London (UK): Humana Press; 2007. p. 103-20.
11. Minn H, Zasadny KR, Quint LE, Wahl RL. Lung cancer: reproducibility of quantitative measurements for evaluating 2-[F-18]-fluoro-2-deoxy-D-glucose uptake at PET. Radiology. 1995; 196:167–73. [PubMed: 7784562]
12. Weber WA, Ziegler SI, Thodtmann R, Hanauske AR, Schwaiger M. Reproducibility of metabolic measurements in malignant tumors using FDGPET. J Nucl Med. 1999; 40:1771–7. [PubMed: 10565769]
13. Grierson JR, Shields AF. Radiosynthesis of 3′-de-oxy-3′-[(18)F]fluorothymidine: [(18)F]FLT for imaging of cellular proliferation *in vivo*. Nucl Med Biol. 2000; 27:143–56. [PubMed: 10773543]
14. Machulla H-J, Blocher A, Kuntzsch M, Wei R, Grierson J. Simplified labeling approach for synthesizing 3′-deoxy-3′-[^{18} F]fluorothymidine ([^{18} F]FLT). J Radioanalyt Nucl Chem. 2000; 243:843–6.
15. Shields AF, Briston DA, Chandupatla S, et al. A simplified analysis of [^{18} F]3′-deoxy-3′-fluorothymidine metabolism and retention. Eur J Nucl Med Mol Imaging. 2005; 32:1269–75. [PubMed: 15991018]
16. Krak NC, Boellaard R, Hoekstra OS, Twisk JW, Hoekstra CJ, Lammertsma AA. Effects of ROI definition and reconstruction method on quantitative outcome and applicability in a response monitoring trial. Eur J Nucl Med Mol Imaging. 2005; 32:294–301. [PubMed: 15791438]
17. Tseng JR, Dandekar M, Subbarayan M, et al. Reproducibility of 3′-deoxy-3′-(18)F-fluorothymidine microPET studies in tumor xenografts in mice. J Nucl Med. 2005; 46:1851–7. [PubMed: 16269599]
18. Kenny L, Coombes RC, Vigushin DM, Al-Nahhas A, Shousha S, Aboagye EO. Imaging early changes in proliferation at 1 week post chemotherapy: a pilot study in breast cancer patients with 3′-deoxy-3′-[(18)F]fluorothymidine positron emission tomography. Eur J Nucl Med Mol Imaging. 2007; 34:1339–47. [PubMed: 17333178]
19. Shankar LK, Hoffman JM, Bacharach S, et al. Consensus recommendations for the use of 18F-FDGPET as an indicator of therapeutic response in patients in National Cancer Institute Trials. J Nucl Med. 2006; 47:1059–66. [PubMed: 16741317]
20. Muzi M, Mankoff DA, Grierson JR, Wells JM, Vesselle H, Krohn KA. Kinetic modeling of 3′-deoxy-3′-fluorothymidine in somatic tumors: mathematical studies. J Nucl Med. 2005; 46:371–80. [PubMed: 15695799]

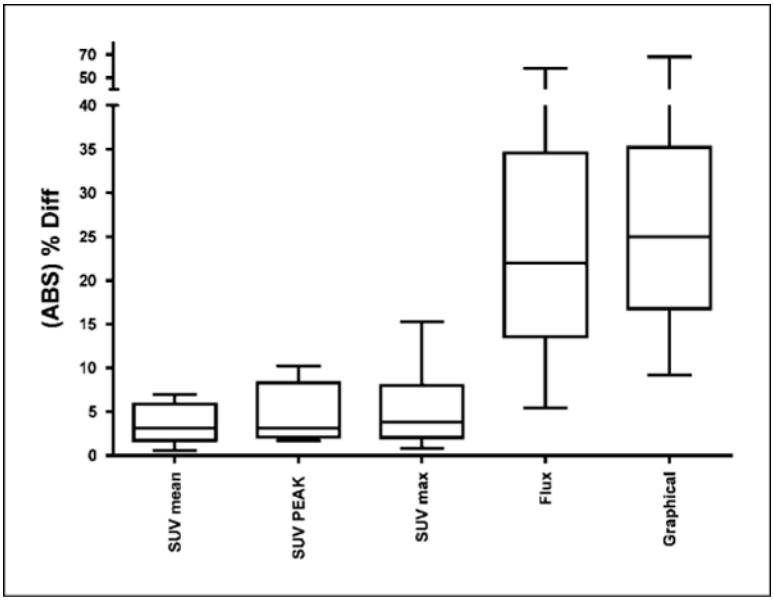

Fig. 1.

Box plot showing the reproducibility (percent difference or percent error) of quantitative FLT approaches using SUV (mean, peak, and maximum) and kinetic measurements.The SUV measurements were obtained from 30 to 60 min. The kinetic measurements were made using the flux determined from a three-compartment model and a graphical approach.The box plot shows the mean percent error (*horizontal line within the box*), the 25th and 75th percentiles (*bottom and top of the box* , respectively), and the range (*bottom and top horizontal bars on the vertical whiskers*).

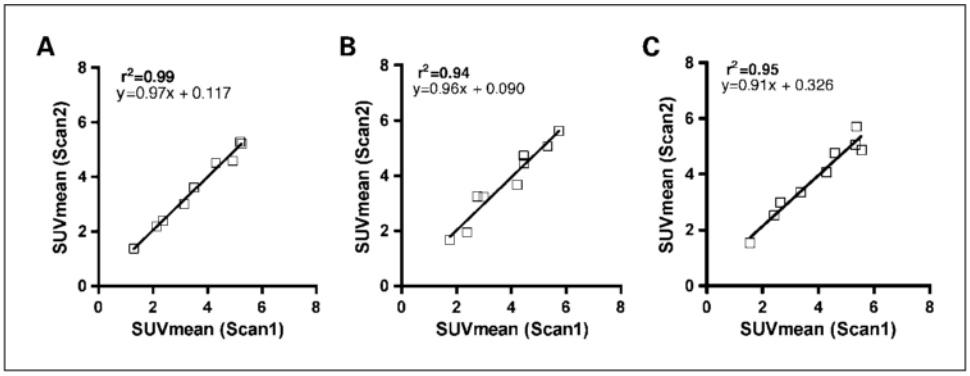

Fig. 2.

SUV_{mean} obtained from scan 1 versus scan 2 obtained from 30 to 60 min (*A*), from 25 to 30 min (*B*), and from 55 to 60 min (*C*) postinjection.

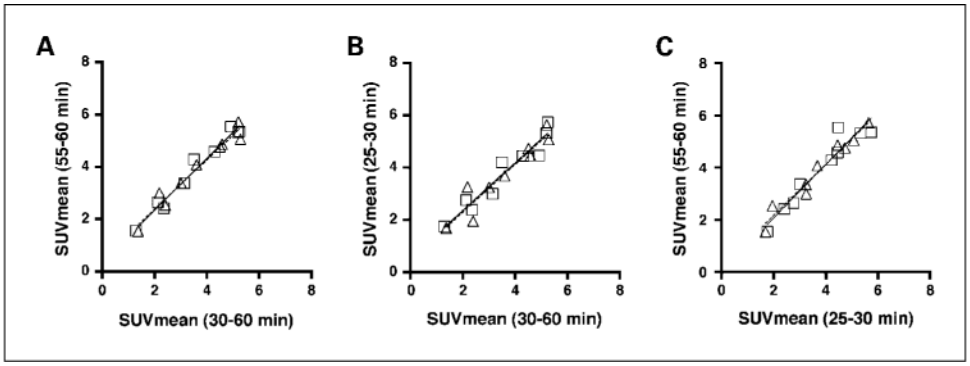

Fig. 3.

SUV_{mean} obtained from all scans ($n = 18$) obtained at 30 to 60 min versus 55 to 60 min (*A*), at 30 to 60 min versus 25 to 30 min (*B*), and at 25 to 30 min versus 55 to 60 min (*C*) postinjection. *Squares* and *solid line*, scan 1; *triangles* and *dotted line*, scan 2.

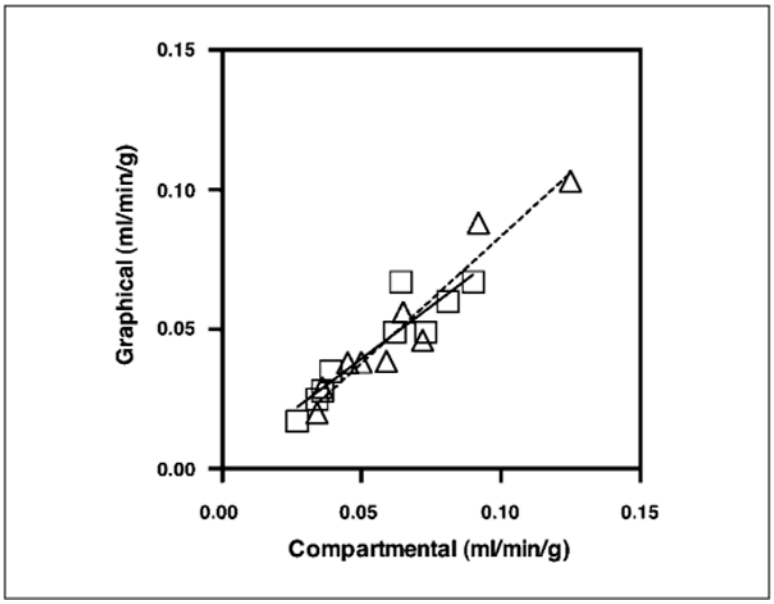

Fig. 4.

Graphical analysis and compartmental analysis for all 18 scans in 9 patients. *Squares* and *solid line*, scan 1; *triangles* and *dotted line*, scan 2.

Table 1

Replicated SUV measurements in patients with lung cancer, comparing SUV_{mean}, SUV_{peak}, and SUV_{max} obtained from 30 to 60 min and SUV_{mean} data obtained from 25 to 30 min and from 55 to 60 min postinjection

Patient	Scans	SUV (30–60 min)			SUV (25–30 min)			SUV (55–60 min)		
		Mean	Peak	Max	Mean	Peak	Max	Mean	Peak	Max
1	1	3.14	3.47	3.65	3.00	3.51	3.91	3.37	3.89	4.28
	2	3.02	3.35	3.68	3.23	3.53	3.93	3.36	3.87	4.29
2	1	5.20	6.44	7.05	5.32	6.32	6.98	5.33	6.62	7.23
	2	5.29	6.29	6.85	5.07	6.05	6.66	5.06	6.16	6.90
3	1	1.29	1.75	1.91	1.75	2.02	2.32	1.55	1.90	2.08
	2	1.38	1.94	2.14	1.68	1.91	2.07	1.54	1.78	2.04
4	1	4.30	5.32	5.52	4.45	5.32	5.56	4.59	5.67	5.96
	2	4.52	5.42	5.69	4.73	5.64	6.12	4.76	5.48	5.82
5	1	4.92	5.49	5.76	4.47	5.03	5.45	5.55	6.12	6.55
	2	4.59	6.08	6.71	4.45	4.99	5.27	4.87	5.48	5.72
6	1	3.50	4.81	5.07	4.21	4.77	5.06	4.29	5.03	5.33
	2	3.61	4.67	4.88	3.67	4.13	4.37	4.08	4.72	5.05
7	1	2.13	2.42	2.52	2.76	3.17	3.43	2.64	3.21	3.46
	2	2.19	2.59	2.64	3.24	3.76	3.97	2.99	3.59	3.74
8	1	5.25	6.82	7.70	5.74	7.07	7.86	5.36	6.70	7.51
	2	5.22	6.65	7.36	5.63	6.70	7.36	5.72	6.84	7.42
9	1	2.36	3.01	3.25	2.39	2.89	3.17	2.42	3.11	3.42
	2	2.40	2.96	3.21	1.94	2.47	2.64	2.53	3.00	3.21

Table 2

Comparison of compartmental and graphical analysis of kinetic data from patients with lung cancer

Patient	Scan	Compartmental flux	Graphical flux
1	1	0.036	0.028
	2	0.065	0.056
2	1	0.073	0.049
	2	0.059	0.038
3	1	0.027	0.017
	2	0.034	0.020
4	1	0.062	0.049
	2	0.050	0.038
5	1	0.064	0.067
	2	0.092	0.088
6	1	0.081	0.060
	2	0.072	0.046
7	1	0.039	0.035
	2	0.045	0.038
8	1	0.090	0.067
	2	0.125	0.103
9	1	0.034	0.025
	2	0.036	0.029

NOTE: Blood input functions were obtained from the aorta and analysis of a blood sample at 60 min was used for metabolite correction.